STUDY OF A SINGLE-BLADE PROPULSION SYSTEM FOR RETRACTABLE ENGINE SAILPLANES

By Paolo Ballocchi; Mario Beretta; Gianni Fumagalli

Presented at the XXV OSTIV Congress, St. Auban, France

Summary

If on one hand aviation moves towards propellers with five, six and more blades, on the other our study is devoted to the use of a single-blade propeller. This apparent contradiction is due to the fact that while in common airplanes the problem is how to discharge in air the higher and higher powers of modern engines, in our technical field the engine must be as light and small as possible so that, once you have retracted it, you don't feel it anymore during the soaring flight. So the small thrust values required by motorgliders and the relatively low powers of the engines make very interesting the use of this kind of propeller with high levels of efficiency, smoothness and simplicity.

Notation and Units

C_T = thrust coefficient
α = flapping angle around the hinge
k = spring torsion coefficient
m_p = blade mass
m_c = counter-weight mass
n = propeller rpm
l_c = counter-weight_CG distance
l_0 = blade thrust application point rotation axes distance
l_p = blade CG rotation axes distance
a = blade axes hinge distance
b = counter-weight hinge distance
Diam = propeller diameter
M = moment around the flapping hinge
Vert = vertical force on the hinge

1. Introduction

The requirement for this project was born when Alisport decided to develop the powered version of its ultralight glider, the Silent.

Notwithstanding, some propulsion units for motorgliders were already present in the market, in October of 1995 when the authors began the study and development of a retractable propulsion system whose main characteristic had to be simplicity. Simplicity means reliability, economy and lightness; hence the choice besides the single blade propeller, the modular trestle frame, the single cylinder engine with a counter rotating balance shaft and the poly-V belt for transmission.

2. Conceptual Solutions of This Single-blade Propeller

Even if already in use in aeolian wind generators and aircraft model fields, no theoretical literature was found. The application of this idea to a manned aircraft required first to understand the physics of the phenomenon and then to write a theory.

In this propeller the lack of other blades entails the need of a counter-weight on the opposite side to the blade. Additionally, the aerodynamic thrust distributed only on the blade needs to be compensated by an off-set position of this counter-weight. At this point the single blade propeller may be designed in equilibrium for a datum thrust value. Since both the aerodynamic and the dynamic forces depend on the square value of propeller rpm, there is a range in which the propeller is balanced. But when the variation in the thrust is due to other parameters, such as blade incidence for gusts or flying speed variation (different TAS or simply during take-off) or, for example, different values of air density, the propeller isn't anymore in equilibrium.

The flapping blade is the patented solution that creates a statically and dynamically stable system of equilibrium of the dynamic forces that follows the variation in the aerodynamic forces when not due to rpm.

In the solution we have used, the whole propeller (that means the blade, the hub and the counter-weight) is flapping. In this way we have obtained:

- functionally the effect on the distance from the two centers of gravity projected in the rotation axes due to a given flapping angle is greater and the equilibrium is reached earlier:
- mechanically all the high dynamic forces are discharged in the hub, which has a conventional blade connection, while the hinge which permits the flapping is loaded only by the thrust and propeller torque.

Figure 1 represents the system at present in use.

3. Analytical Point of View

The hypothesis formulated in the preliminary phase have to be quantified with an analytical approach.

$$M(\alpha,C_T) = -k\alpha - m_p(2n\pi)^2\left[l_p\left(1-\frac{a^2}{2}\right)-a\alpha\right]\frac{a-l_0\alpha}{l-\frac{a^2}{2}} + m_c(2n\pi)^2\left[ba+l_c\left(1-\frac{a^2}{2}\right)\right]\left[b\left(1-\frac{a^2}{2}\right)-l_c\alpha\right] + \rho n^2 Diam^4 C_T l_0 \quad (1)$$

$$Vert(\alpha,C_T) = (2n\pi)^2\left[a^2\left(m_c\frac{l_c}{2}-m_p\frac{l_p}{2}\right)-a\left(\frac{\rho Diam^4 C_T}{4\pi^2}+am_p+bm_c\right)\right] \quad (2)$$

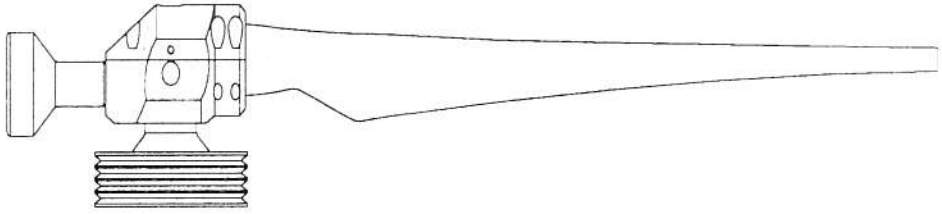

Figure 1. Drawing of the blade unit, composed by the avional integrated hub-keeper pulley, the stainless-steel counterweight, the avional hub and the carbon fiber blade.

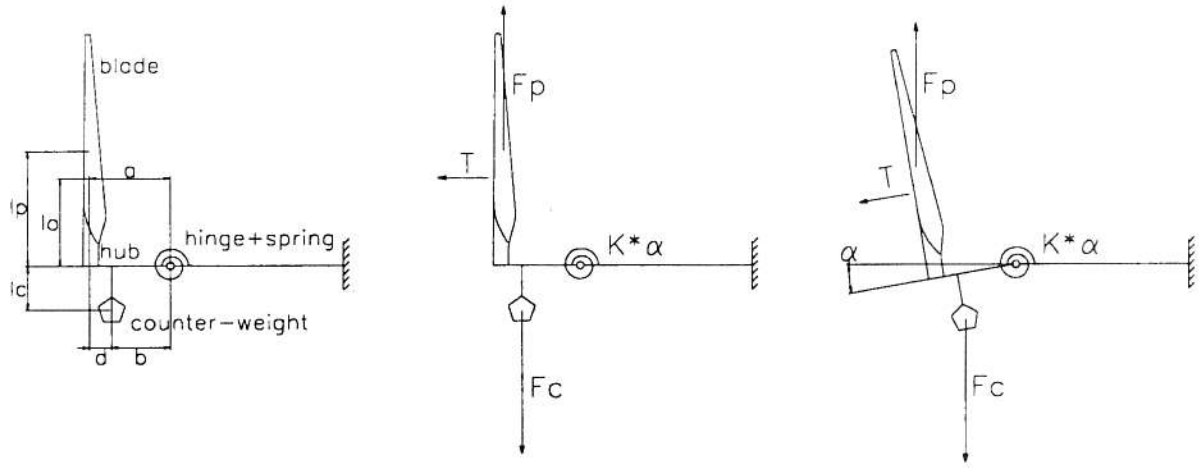

Figure 2. The sketch is the single-blade propeller viewed in the plane perpendicular to the flapping hinge, where α is the flapping angle with postitive values as shown.

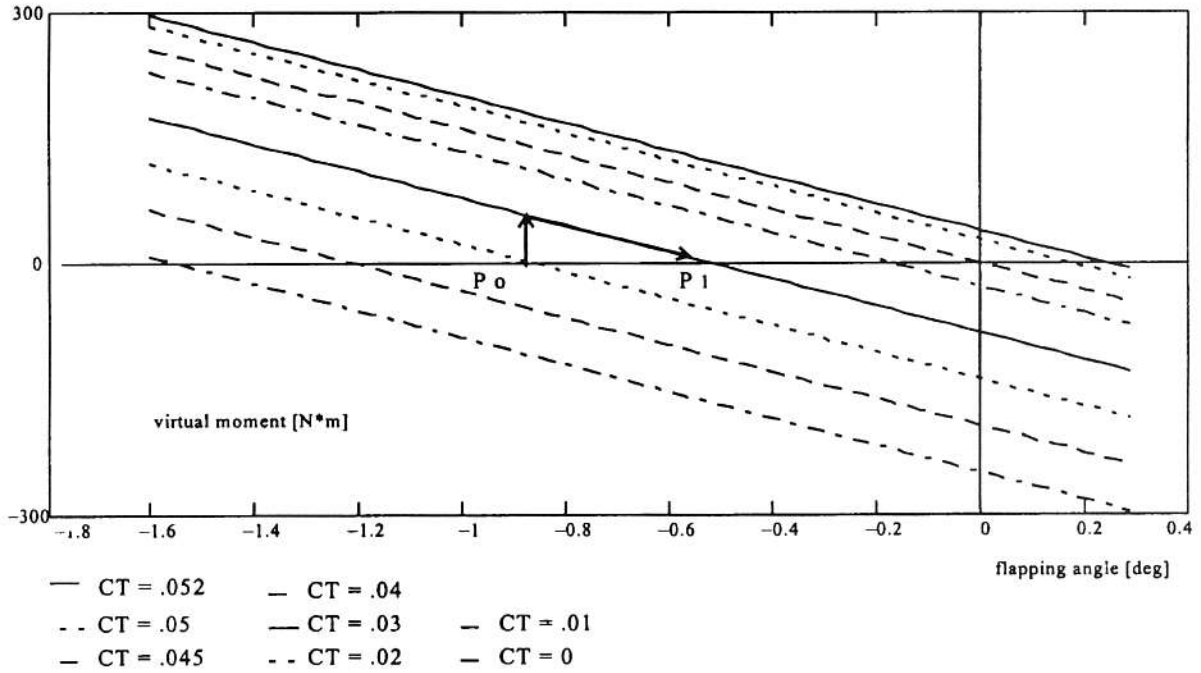

Figure 3. The straight lines represent the moment around the hinge values of the system in the hypothetical fixed a value: the arrows represent how the system actually adapts itself to the C_T variation, always working in the axes M = 0.

Considering the plane perpendicular to the flapping hinge, as in Figure 2, we can write the equations (l) and (2) that regulate the phenomenon. They represent the vertical forces and moment around the hinge equilibrium and are written with linear trigonometric functions, since the angle a is close to 0.

Let's now consider the graphs reported in Figure 3 and Figure 4 that represent an abstract of calculated results.

With the first graph it can be seen that the stable response of the unit is achieved; when flight condition variation brings a C_T variation the system answers adapting the flapping angle. In an infinitesimal C_T range the system behaves, as shown in the example by the arrows, moving from a point P_0 (α_0, 0) to a second point P_1 (α_1, 0), both of them with a 0 moment transmitted to the structure.

But if the propeller cannot transmit moments through a hinge, the vertical force disturbance can pass through this connection; so the second graph (Figure 4) can be considered the main quantification of disturbances induced by the use of a hinge connection with a single-blade propeller. The envelope curve shows the resultant vertical force that loads the propeller shaft at values physically determined by the moment of equilibrium with the C_T value used in that flight condition. This curve is a function of the hub geometry and, as a result of our project, presents its best characteristics for the C_T range commonly in use (the continuous C_T envelope curve in the graph). Beyond this optimized range, it must be noted how the maximum

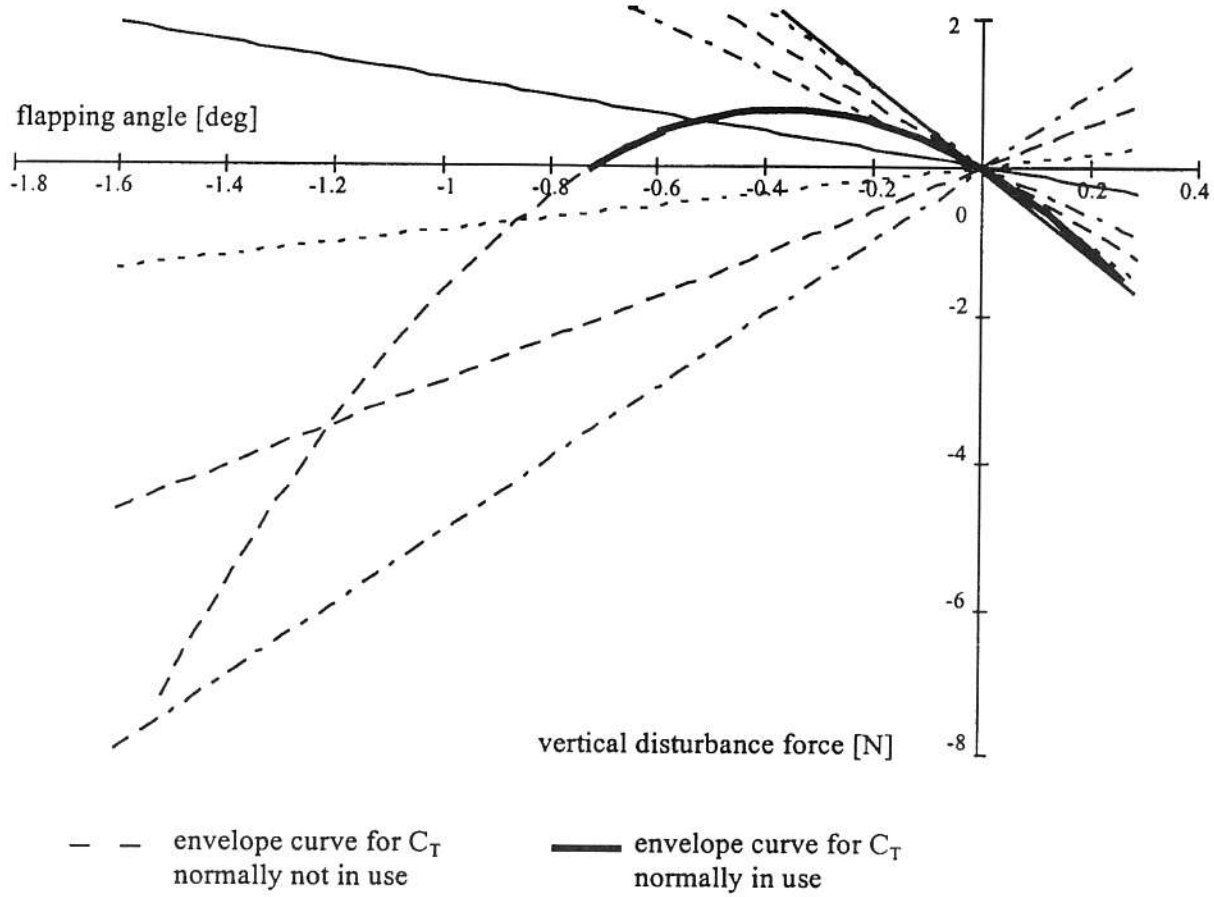

Figure 4. The straight lines represent the vertical force that pass through the hinge to the structure and are virtual; their C_T values are the same as Figure 3. The correspondence between the 'M = 0' α values of Figure 3 and the lines of this graph at the same C_T are represented by the envelope curves and give the real disturbance force of this system.

vertical force for the C_T range actually not used in motorgliders (the dashed envelope curve) is no more than 8 Newtons, practically corresponding to a mass variation of 1/10 gram at the blade tip.

In regards to the drag of the blade, it is much greater than the counter-weight drag and potentially the source of undesired disturbances. The problem has been solved by moving the counter-weight axes out of alignment with the blade axes. The algorithms studied for the thrust has been applied except for the possibility of flapping in that direction, since the propeller would became unstable from the aero-elastic point of view. So a mixed theoretical-empirical system has been performed to obtain the final balancing, thereby introducing transverse forces of known and irrelevant amplitude.

4. Experimental Phase

The numerical values found during the analysis, whose main lines have been just reported, and all the structural hypothesis (conceptual and finite-element-analysis models) had to be verified during laboratory, bench and flight tests.

To check the algorithms for the design of the hub, several measurements during bench tests were done. In particular accelerometers were installed in different positions of the trestle frame to experimentally quantify the vibrations of the unit. The final result in the frequency domain can be observed in the graph of Figure 5 and in Table 1.

To correctly compare the vibration values reported, it must be kept in mind that;

- the engine in use is equipped with counter-rotating shaft;
- the measurements, to whom Figure 5 refers, were done with the accelerometer nearer to the propeller axes than to the engine thereby quantifying the vibration with its speed.

Hence, it is remarkable to verify how the vibration level of the propeller is lower than the first and second order vibrations of the equilibrated engine.

As regards the flight tests, one of the most particular

frequency	*velocity*	*notes*
[rpm]	[mm/sec]	
3014	38.44	propeller
5214	46.28	engine rpm and 1° order engine
10420	59.56	2° order engine

Table 1. Peak values of the graph reported in Figure 5..

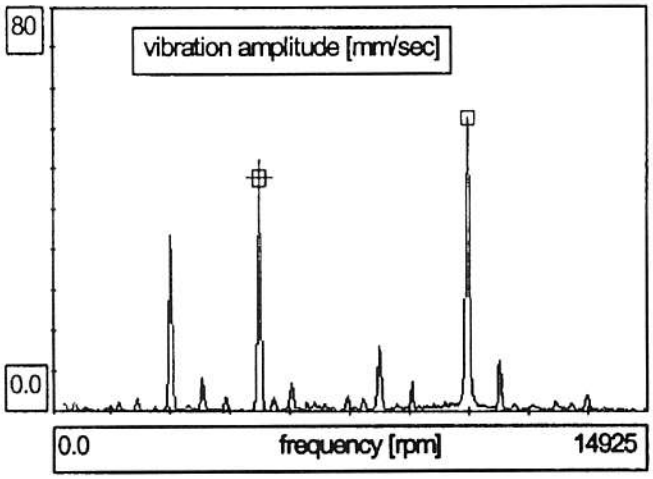

Figure 5. Vibration quantities in the frequency domain.

behaviors encountered has been the counter-weight wake effect on the blade. As a function of its shape and length, the propeller rpm accelerates when performing static thrust since the most twisted part of the blade remains in the counter-weight wake. This behavior has two main effects:

- the static thrust lift distribution on the blade is not the free air theoretical one and its barycenter is more distant from the rotation axes than when the aircraft is in normal flight and the blade is out of any wake. This feature creates a greater moment and the propeller needs an increment in the flapping angle to equilibrate the lift moment in this condition;
- when performing static thrust, the propeller and hence the engine can reach a higher rpm at a fixed point. This results in achieving high values of power and thrust from the beginning of take-off while maintaining a substantially constant rpm from 0 to 100 km/h.

Conclusions

After 15 months of study and evolutions, in December of 1996,the "Silent monopala" equipped with the single-blade propeller made its first flight. The innovative aspect of the solution can be seen in the following photograph, Figure 6.

At present, the development, fatigue bench and flight tests are in progress. Relevant to this experience, we can say that, besides the simplicity and reduced size advantages, the single blade system has performed a static thrust/power ratio of more than 4 kg_f/horsepower with a 1.4 m diameter propeller. What more amazes the test pilots is the great operating smoothness of this unit when compared with the present state-of-the-art motorgliders.

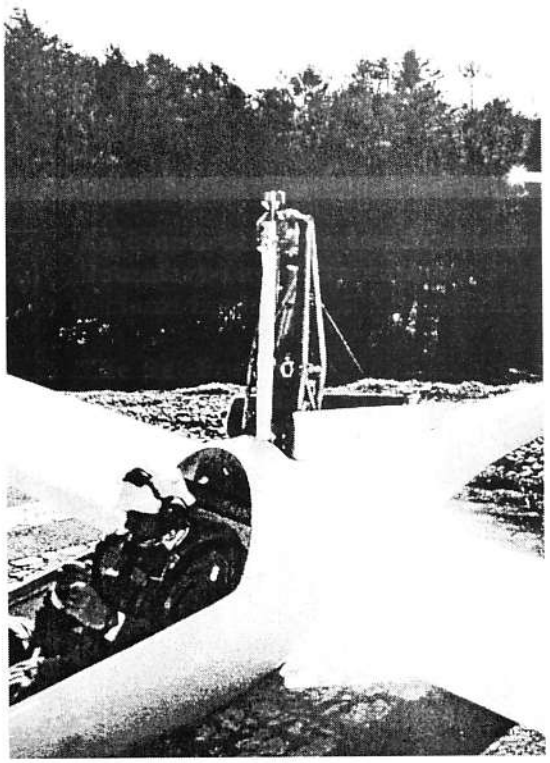

Figure 6. Leonardo Brigliadori test pilot at the first flight.

6. Acknowledgments

We want to sincerely thank each person who worked on this project, both in the theoretical and practical phase.

A particular acknowledgment goes to Tecom personnel for their work and to Walter Mauri for his contribution.